Strahlenther Onkol (2020) 196:182–192
https://doi.org/10.1007/s00066-019-01549-z

ORIGINAL ARTICLE

A novel approach to SBRT patient quality assurance using EPID-based real-time transit dosimetry

A step to QA with in vivo EPID dosimetry

Christos Moustakis[1] · Fatemeh Ebrahimi Tazehmahalleh[2] · Khaled Elsayad[1] · Francis Fezeu[3] · Sergiu Scobioala[1]

Received: 19 March 2019 / Accepted: 26 October 2019 / Published online: 10 January 2020

Abstract

Purpose Intra- and inter-fraction organ motion is a major concern in stereotactic body radiation therapy (SBRT). It may cause substantial differences between the planned and delivered dose distribution. Such delivery errors may lead to medical harm and reduce life expectancy for patients. The project presented here investigates and improves a rapid method to detect such errors by performing online dose verification through the analysis of electronic portal imaging device (EPID) images.

Methods To validate the method, a respiratory phantom with inhomogeneous insert was examined under various scenarios: no-error and error-simulated measurements. Simulation of respiratory motions was practiced for target ranges up to 2 cm. Three types of treatment planning technique – 3DCRT (three-dimensional conformal radiation therapy), IMRT (intensity modulated radiation therapy), and VMAT (volumetric modulated arc therapy – were generated for lung SBRT. A total of 54 plans were generated to assess the influence of techniques on the performance of portal dose images. Subsequently, EPID images of 52 SBRT patients were verified. Both for phantom and patient cases, dose distributions were compared using the gamma index method according to analysis protocols in the target volume.

Results The comparison of error-introduced EPID-measured images to reference images showed no significant differences with 3%/3 mm gamma evaluation, though target coverage was strongly underestimated. Gamma tolerance of 2%/2 mm reported noticeable detection in EPID sensitivity for simulated errors in 3DCRT and IMRT techniques. The passing rates for 3DCRT, IMRT, and VMAT with 1%/1 mm in open field were 84.86%, 92.91%, and 98.75%, and by considering MLC-CIAO + 1 cm (threshold 5%), were 68.25%, 83.19%, and 95.29%, respectively.

Conclusion This study demonstrates the feasibility of EPID for detecting the interplay effects. We recommend using thin computed tomography slices and adding sufficient tumor margin in order to limit the dosimetric organ motion in hypofractionated irradiation with preserved plan quality. In the presence of respiratory and gastrointestinal motion, tighter criteria and consequently using local gamma evaluation should be considered, especially for VMAT. This methodology offers a substantial step forward in in vivo dosimetry and the potential to distinguish errors depending on the gamma tolerances. Thus, the approach/prototype provides a fast and easy quality assurance procedure for treatment delivery verification.

Keywords Electronic portal imaging device · Stereotactic body radiation therapy · Quality assurance · In vivo dosimetry · Real time transit dosimetry

These authors contributed equally to this work: C. Moustakis, F. Ebrahimi Tazehmahalleh.

✉ Christos Moustakis
christos.moustakis@ukmuenster.de

[1] Department of Radiation Oncology, University Hospital Muenster, Muenster, Germany

[2] Department of Radiation Oncology, University Hospital of Cologne, Cologne, Germany

[3] Department of Neurology, Mittelmosel Clinic, Zell, Germany

Introduction

Hypofractionated radiotherapy requires high precision. Access to additional imaging modalities increases tumor control probability while simultaneously reducing normal tissue complications [1, 2]. These provide the opportunity to escalate the dose to the tumor and apply hypofractionated stereotactic body radiation therapy (SBRT). Increasing requests for high-definition modulated therapy procedures puts stress on patient-specific plan quality assurance (QA) resources. Therefore, it is essential to effectively monitor the target to ensure that the tumor is within the beam aperture.

Research has illustrated that clinically approved plan quality can differ significantly [3–10]. Pre-treatment QA usually verifies the accuracy of delivery for individual plans. However, traditional pre-treatment QA is not able to detect changes in patient anatomy and there is still the possibility of systematic and random delivery uncertainties between/during each fraction. These types of uncertainties are unique to each fraction. They include undetected machine errors, patient weight gain/loss, inadequate immobilization, tumor growth/response, normal tissue shrinkage, and human errors (accidental plan modification, incorrect treatment site or plan/patient, etc.). All of these uncertainties can be detected by in vivo dosimetry [11–13]. More accurate patient setup can be achieved by several imaging techniques. Nevertheless, when dealing with dynamic tumors, difficulties are still encountered with 3D matching in terms of clearly depicting the tumor and identifying and reproducing its location [14].

Studies on tumor motion reported the majority of respiration movements to happen in the superior–inferior (SI) direction, especially the lower lobe of the lung exhibits the most considerable amount of motion [15, 16]. This affects treatment accuracy and reduces patient setup reproducibility [17, 18]. Longer treatment time is linked to a substantial risk of intra-fractional motion, as well as variations between imaging and treatment time. In addition, this can produce hot/cold spots [19]. Therefore, transit dosimetry can play a key role in the verification procedure chain. To some extent, the quality and safety of treatment have been investigated by a widely available electronic portal imaging device (EPID) [20, 21]. These studies have shown remarkable advantages for modern dynamic delivery techniques as well as for hypofractionated deliveries [22–26]. International Atomic Energy Agency Human Health Report No. 8 reported several treatment errors utilizing in vivo entrance/exit dosimetry during treatment [27]. Some errors during three-dimensional conformal radiation therapy (3DCRT) and intensity-modulated RT (IMRT) that could not be noticed by pre-treatment QA were detected by means of EPID-based in vivo dosimetry [28]. This study aims to check the ability of EPID in detecting dose delivery errors and verify its sensitivity. In this context, inter- and intra-fractional motion management were investigated by implementing hypofractionated treatment. The detectability threshold of the process was studied under comparisons of improved and local gamma index method using different analysis protocols for various delivery techniques.

Materials and methods

Phantom study and treatment delivery

A dynamic 4D phantom, QUASAR™ programmable respiratory motion platform (Modus Medical Devices, Ontario, Canada), was used to verify the uncertainties of EPID tracking. The phantom was composed of cedar insert (cylinder) containing a water-equivalent ball 3 cm in diameter that moves in superior–inferior directions as shown in Fig. 1. Computed tomography (CT) images were acquired with 1, 2, and 3 mm slice thicknesses to determine the optimal slice thickness. American Association of Physicists in Medicine (AAPM) Report No. 91 recommends that respiratory motion should be considered when tumor movement exceeds 5 mm. On the contrary, a superior–inferior tumor movement

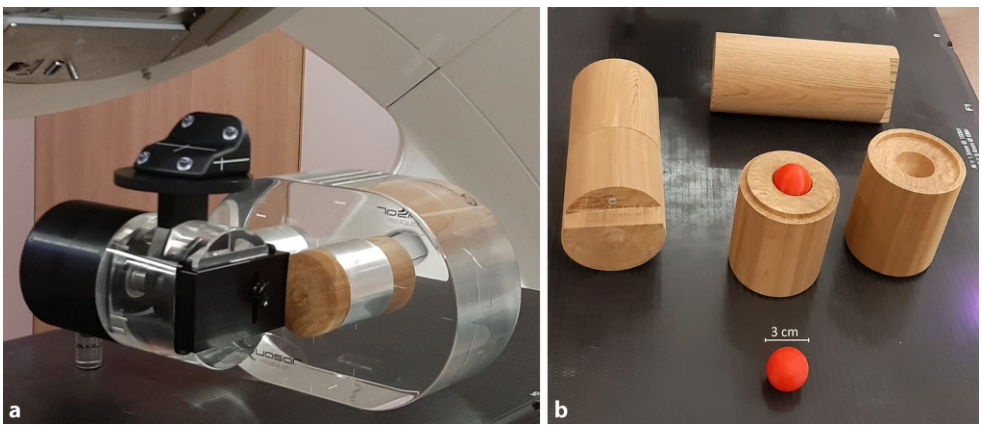

Fig. 1 **a** QUASAR™ programmable respiratory motion phantom (Modus Medical Devices, Ontario, Canada) with **b** cedar lung insert in which an offset polystyrene target 3 cm diameter is embedded

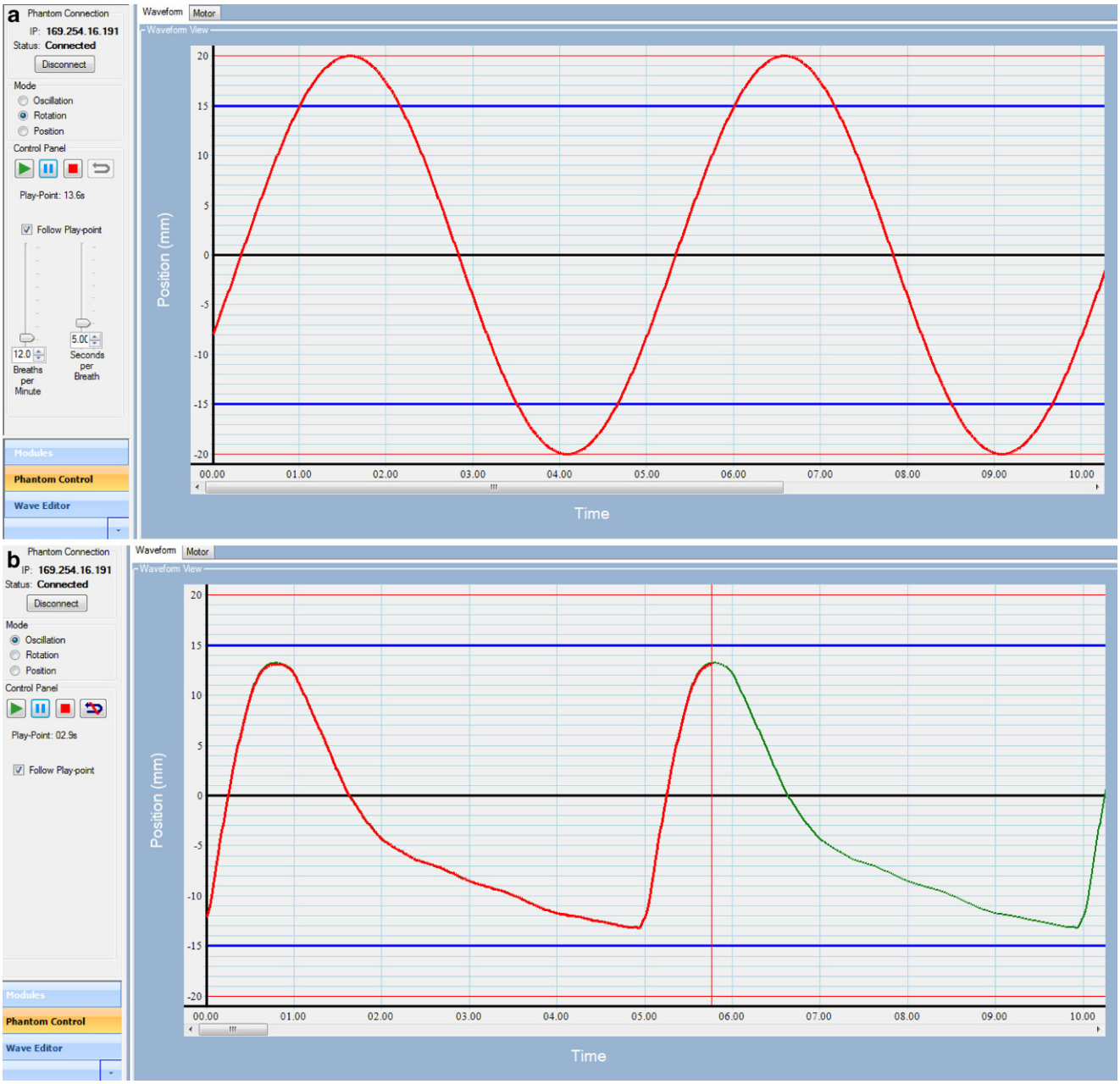

Fig. 2 Screenshots of respiratory gating controlled by scanner software for phantom measurements. **a** sinusoidal curve with amplitude of 2 cm and 5 s per breathing cycle, **b** a natural respiratory curve with amplitude of 1.3 cm and 5 s per breathing cycle

more than 2 cm is relatively unusual [29]. Consequently, 4DCT scans were executed in different motion phases. The first phase was by applying a sinusoidal pattern with peak amplitude of ±20, ±10, ±5, and 0 mm. The period for breathing cycle was constant for all amplitudes. The second phase was based on a predefined natural respiratory rhythm in oscillation mode with 13 mm and 20 mm motion amplitude. Fig. 2 shows screenshots of a sinusoidal pattern for 20 mm and a natural breathing for 13 mm peak amplitude. A total of 18 CT scans were created. 4DCT imaging was used to generate ITV and in accordance with the RTOG 0915 protocol, the planning target volume (PTV) was then created by expanding a uniformly isotropic 3 mm margin from the ITV.

3DCRT, sliding-window IMRT, and volumetric-modulated arc therapy (VMAT) plans were created in each breathing cycle for each CT slice thickness. All plans were generated with a 10-MV flattening filter-free (FFF) beam using a dose rate of 2400 MU/min. Three-field 3DCRT plans with gantry angles of 0°, 240°, and 280°, also for IMRT a three-field plan with 230°, 270°, 330° angles, were generated. Double-arc VMAT treatment plans were created

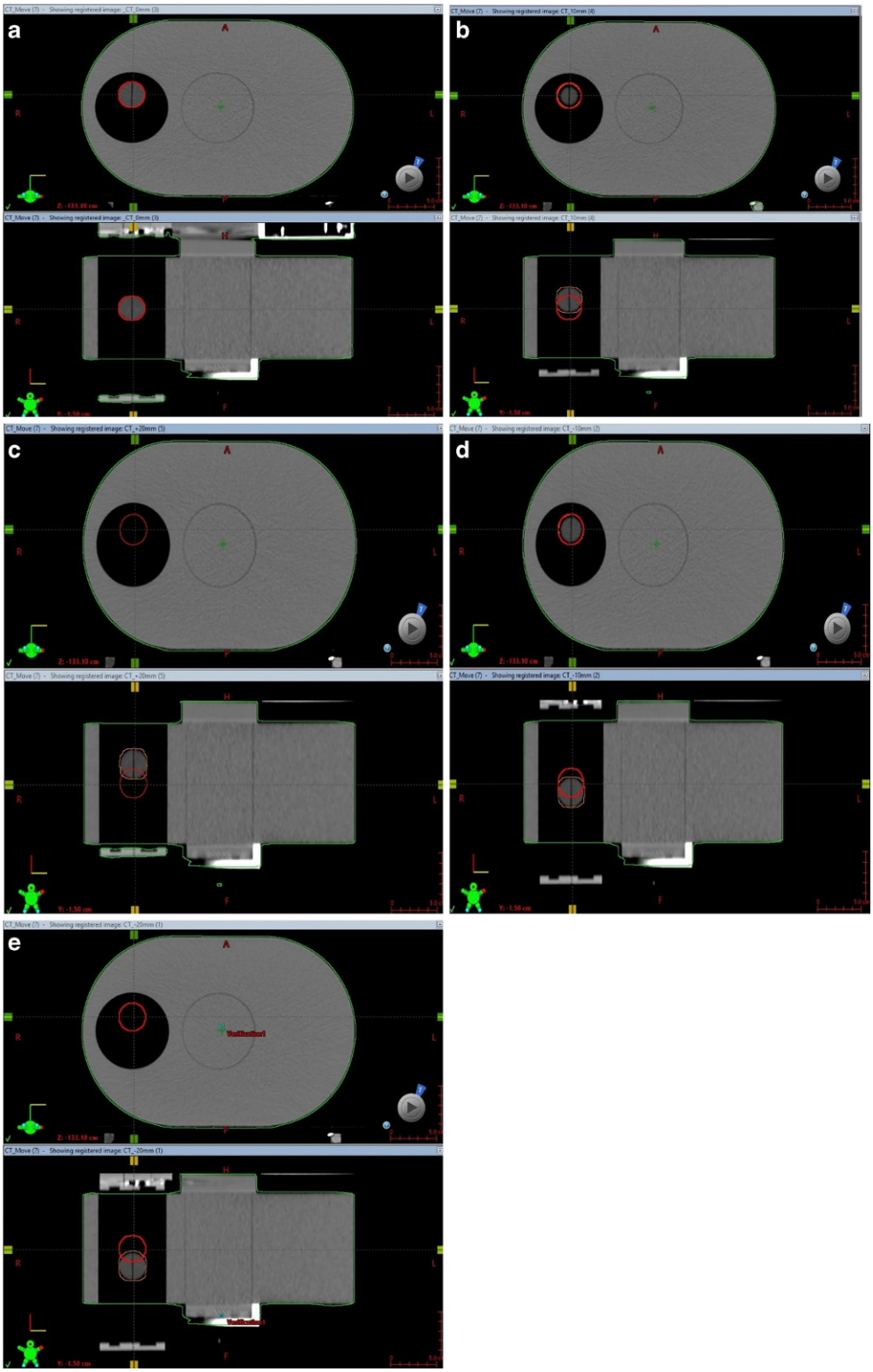

Fig. 3 Target structure motion, ranging from 0 (**a**) to 2 cm (**e**). In general, as the range of motion increases, the CT value within the PTV (*red circle*) decreases

for gantry rotation angles of 0° until 180° and vice versa. All 54 plans were calculated in the Eclipse Treatment Planning System (Version 15.5, Varian Medial Systems, USA) using the Analytical Anisotropic Algorithm (AAA) with 1.25 mm calculation resolution. Treatment was delivered with a Varian TrueBeam linear accelerator equipped with an amorphous silicon flat panel (aS1000; Varian Medical Systems, CA). A direct comparison of the target positions in each breathing phase versus the static position are illustrated in Fig. 3.

Table 1 Demographic characteristics of patients

Characteristic		Number
Sex	Male	25
	Female	13
Age (years)	Median	68
	Range	16–88
Primary tumor location	Lung	28
	Liver	16
	Mediastinum	2
	Lymph nodes	2
Primary tumor size (cm)	Median	3.3
	Range	1.4–8.9
Planning target volume (cm^3)	Median	18.37
	Range	1.69–363.07
Total lung volume (cm^3)	Median	3372.73
	Range	1625.21–7009.68
Total liver volume (cm^3)	Median	1392.56
	Range	937.63–2429.63

Patient selection and planning

Retrospective data were collected from patients with lung or liver lesion who underwent SBRT between 2010 and 2017. The clinical cases were chosen randomly from each tumor size category to explore the difference in treatment delivery for different tumor sizes. Patient characteristics are summarized in Table 1. During CT simulation, patients were immobilized with the BlueBAG™ BodyFix® cushions (Elekta, Stockholm, Sweden) vacuum system. The gross tumor volume was determined for lung lesions using the lung and for liver lesions using the soft tissue window, as described in the International Commission on Radiation Units and Measurements Report 91 [30]. The German Society of Radiation Oncology (DEGRO) guideline recommends contrast-enhanced CT scans or, ideally, contrast-enhanced magnetic resonance imaging (MRI) to define target volumes in liver lesions [31]. All patients underwent either four-dimensional CT (4DCT; $n=10$) or 4D positron-emission tomography-CT (PET-CT; $n=42$) to quantify respiratory motion and to delineate the internal target volume (ITV). This accommodated for displacements of the target volume occurring during respiratory and cardiac motion. Subsequently, the ITV was enlarged by 3 mm to initiate a PTV. Irradiation was delivered via photon energies of 6-MV and 15-MV FF (flattening filter) beam with dose rate of 600 MU/min or a 10-MV FFF (flattening filter free) beam with maximum dose rate of 2400 MU/min. Most patient plans were generated with 10-MV FFF and VMAT; this is the used beam quality for SBRT in our institute. Thus, the data for other techniques and energies were excluded from the study. Treatment prescriptions were 37.5 Gy in three fractions with 65% surrounding isodose or 35 Gy in five for patients who could not tolerate the prescribed dose. So, 52 generated VMAT plans were with 2 arcs ($n=43$), 1 arc ($n=6$), and 3 arcs ($n=3$). Prior to each fraction, patients were localized with free-breathing cone beam CT (FBCBCT) and registered with the free-breathing planning CT (average 4DCT). Therefore, tumor-based registration is used as a registration parameter for the CBCT. A pre-treatment verification was performed for all patients' treatment plans according to clinical routine, with a 2D-Array (I'mRT MatriXX, IBA Dosimetry). In addition, the monitor units were double checked with the commercially available independent software RadCalc (Lifeline Software Inc., v6.2 Build 5.3).

EPID image acquisition

The sensitive area of the imager is $40\times30\,cm^2$ with 1024×768 resolution (0.392 mm^2 pixels). The panel was calibrated according to the vendor's specifications with standard dark field, flood field, diagonal beam profile correction, and absolute dose calibration. EPID response was scaled such that one calibrated unit corresponds to 100 MU delivered by a $10\times10\,cm^2$ open field at 100 cm SSD. Calibration validation was done in weekly routine. When the dose feedback difference was larger than 2%, a new calibration was carried out.

In order to evaluate EPID sensitivity and specificity in detecting inter- and intra-fractional motions, patient-related errors were simulated on the phantom. Intentional errors were introduced by shifting the target during treatment delivery. Target position was modified in each fraction by –20, –10, –5, 0, 5, 10, and 20 mm in an SI direction. The introduced shifts were either larger or smaller than the move-

ment of the target in the baseline (no error) plan. Therefore, the performance of EPID on error detection for large tumor shifts or shrinkage was tested. EPID images were acquired for all baseline plans and error-introduced plans per individual arc/field (a total of 162) in each fraction.

The clinical workflow for patients who underwent verification varied minimally from regular patients. During the treatment, the EPID was set to acquire.

EPID image analysis

To incorporate the effect of inter-setup and target motion, each fraction was delivered after introducing the inter-target motion. EPID images from the baseline plan for the phantom study as well as the image from the first treatment fraction of the patient study were used as reference images. The clinical impact of the errors was analyzed with dedicated ARIA™ portal vision software within the Eclipse™ Treatment Planning System (Version 15.5, Varian Medial Systems, USA). In each case, the error-introduced EPID-measured images were compared to the baseline (no error) images using gamma analysis. The gamma-index method quantitatively evaluates the similarity of two dose distributions, point by point, using dose differences (DD) combined with distance-to-agreements (DTA) and the gamma criterion. In order to assess the effects of the modifications, local and improved gamma passing rates (%GP) between the no-error and error-simulated measurements were evaluated. In the older algorithm (global), for DD, the system only considered integer pixel positions around the pixel being evaluated. According to the Varian portal dosimetry (PD) reference guide, this sampling limitation may result in overestimation of the gamma value at the evaluation point. Therefore, the improved option allows the evaluation to interpolate between neighboring points. Three sets of gamma criteria using 1%/1 mm, 2%/2 mm, and 3%/3 mm were investigated. In transitioning to PD, we need to determine how to define the region of interest (ROI) for analysis. For all criteria, three approaches to define the region of interest were employed: field, MLC complete irradiation area outline (CIAO) + 1 cm and MLC-CIAO + 1 cm with a threshold of 5% of maximum dose. MLC-CIAO + 1 cm corresponds to the opening envelope of the MLC incremented by 1 cm. The regions with doses higher than 5% of the maximum dose (low-dose threshold) and the area of MLC-CIAO were included to investigate the influence of low doses on the gamma parameters. A field/arc was clinically acceptable if at least 95% of its points got a gamma score under one (pass the gamma test). Other parameters were also checked to observe complications on the beams, but were not used as a pass/fail criterion (parameters such as gamma map, average gamma, maximum gamma, area gamma >0.8, and area gamma >1.2). The nonparametric statistical Friedman

Table 2 Median improved gamma passing rate for individual fields in 3DCRT and IMRT-SBRT plans. EPID images were assessed in different acceptance criteria. A lower gamma pass rate number indicates greater sensitivity to error detection

Technique	Irradiation field	Gamma criteria (area gamma <1)								
		3%/3 mm			2%/2 mm			1%/1 mm		
		ROI								
		Field	*MLC-CIAO + 1 cm*	*MLC-CIAO + 1 cm (threshold 5%)*	*Field*	*MLC-CIAO + 1 cm*	*MLC-CIAO + 1 cm (threshold 5%)*	*Field*	*MLC-CIAO + 1 cm*	*MLC-CIAO +1 cm (threshold 5%)*
3DCRT	1	96.8	96.27	93.47	93.3	92.13	86.3	83.57	80.73	66.33
	2	98.2	97.93	96.6	93.13	91.97	86.86	84.73	82.2	70.93
	3	96.77	95.9	92.4	93.33	91.53	84.43	86.1	82.43	67.5
IMRT	1	98.87	98.57	96.97	97.4	96.73	92.33	93.97	91.67	84.47
	2	99.33	99.13	98.3	97.5	96.83	93.87	93.03	91.27	83.07
	3	98.83	98.57	96.87	97.4	96.73	93.07	93.83	92.2	83.33
	4	99.2	99	97.87	97.17	96.5	92.37	93.27	91.63	81.9

ROI Region of Interests, *MLC-CIAO* multi leaf collimator – complete irradiation area outline, *3DCRT* three-dimensional conformal radiation therapy, *IMRT* intensity modulated radiation therapy

two-way analysis of variance by ranks was used to evaluate the data.

Results

A small tumor volume (CTV: 3.26 cm^3, PTV: 5.37 cm^3) was purposely chosen for phantom measurements to evaluate the feasibility of EPID-based real-time transit dosimetry for small fields.

To estimate the dose distribution in the target volume for baseline plans, the phantom was irradiated in 18 fractions. Each irradiation modality included motion simulation (–20, –10, 10, 20 mm) in the SI direction, normal breathing rhythm, and a static reference condition. One hundred and sixty-two EPID images from baseline plans were collected for all CT series. The results were evaluated in terms of gamma index ($\Gamma_{3\%/3\,mm,\ 2\%/2\,mm,\ 1\%/1\,mm}$), which is calculated using spatial and dosimetric limits of DTA and dose difference. Table 2 summarizes the %GPs for all measured fields in 3DCRT and SW-IMRT to investigate the ability of EPID error detection. It shows the median improved gamma pass rates between no-error and error-introduced SBRT plans. Overall, %GPs were reduced slightly by 3%/3 mm, 2%/2 mm, and 1%/1 mm criteria. The majority of simulated errors were detected with a gamma tolerance of 1%/1 mm. A lower gamma pass rate number indicates greater sensitivity to error detection. 3%/3 mm criteria with MLC-CIAO + 1 cm threshold 5% showed a slightly lower pass rate in 3DCRT plans but not significant enough to discriminate errors. More significant reduction happened with tighter criteria. The motion induced-errors could be detected with 2%/2 mm by any opening envelopes analysis protocol in 3DCRT fields. The rather loose criteria could not detect any induced intentional errors by IMRT plans. The improved gamma pass rate of 95% with 2%/2 mm considering MLC-CIAO + 1 cm (threshold 5%) criteria could manifests changes for each introduced-error measurements in IMRT technique.

Table 3 presents the median improved/local gamma pass rates for EPID measurements in VMAT plans. Each improved %GPs criterion showed no significant difference in analysis (median = 98.79, range: 95.1–99.93). By varying the analysis protocol from 1%/1 mm/improved to 1%/1 mm/local and considering the tighter area of MLC-CIAO + 1 cm (threshold 5%), the error detection sensitivity of EPID could be significant. Results showed that EPID-based error detection depends strongly on the gamma evaluation method and the acceptance criteria. The correlation between the selected gamma tolerances and detected error magnitude was based on the average gamma pass rate. For example, if non-stringent gamma criteria are used (as reported in Tables 2 and 3), treatment plans would pass the gamma evaluation even though target displacement was added up to 2 cm in maximum. Fig. 4 represents the comparison of EPID-measured images between the first fraction and one

Table 3 The results indicate the fraction's median pass rate under different gamma criteria in VMAT. Motion patterns were induced on the QUASAR™ phantom (MODUS, London, Ontario Canada) and target dose distribution was compared to the planned dose distribution

				Arcs	
				1	2
Gamma criteria (area gamma <1) protocol DD/DTA	Improved gamma	3%/3 mm	*Field*	99.8	99.93
			MLC-CIAO + 1 cm	99.63	99.9
			MLC-CIAO + 1 cm (threshold 5%)	99.1	99.7
		2%/2 mm	*Field*	99.63	99.8
			MLC-CIAO + 1 cm	99.27	99.67
			MLC-CIAO + 1 cm (threshold 5%)	98.27	99.23
		1%/1 mm	*Field*	98.93	98.83
			MLC-CIAO + 1 cm	98.1	97.87
			MLC-CIAO + 1 cm (threshold 5%)	95.47	95.1
	Local gamma	3%/3 mm	*Field*	99.8	99.93
			MLC-CIAO + 1 cm	99.63	99.9
			MLC-CIAO + 1 cm (threshold 5%)	99.1	99.77
		2%/2 mm	*Field*	99.6	99.8
			MLC-CIAO + 1 cm	99.26	99.63
			MLC-CIAO + 1 cm (threshold 5%)	98.23	99.63
		1%/1 mm	*Field*	97.3	97.1
			MLC-CIAO + 1 cm	95.03	94.77
			MLC-CIAO + 1 cm (threshold 5%)	88.13	88.17

MLC-CIAO multi leaf collimator – complete irradiation area outline, *DD* dose difference, *DTA* distance to agreement

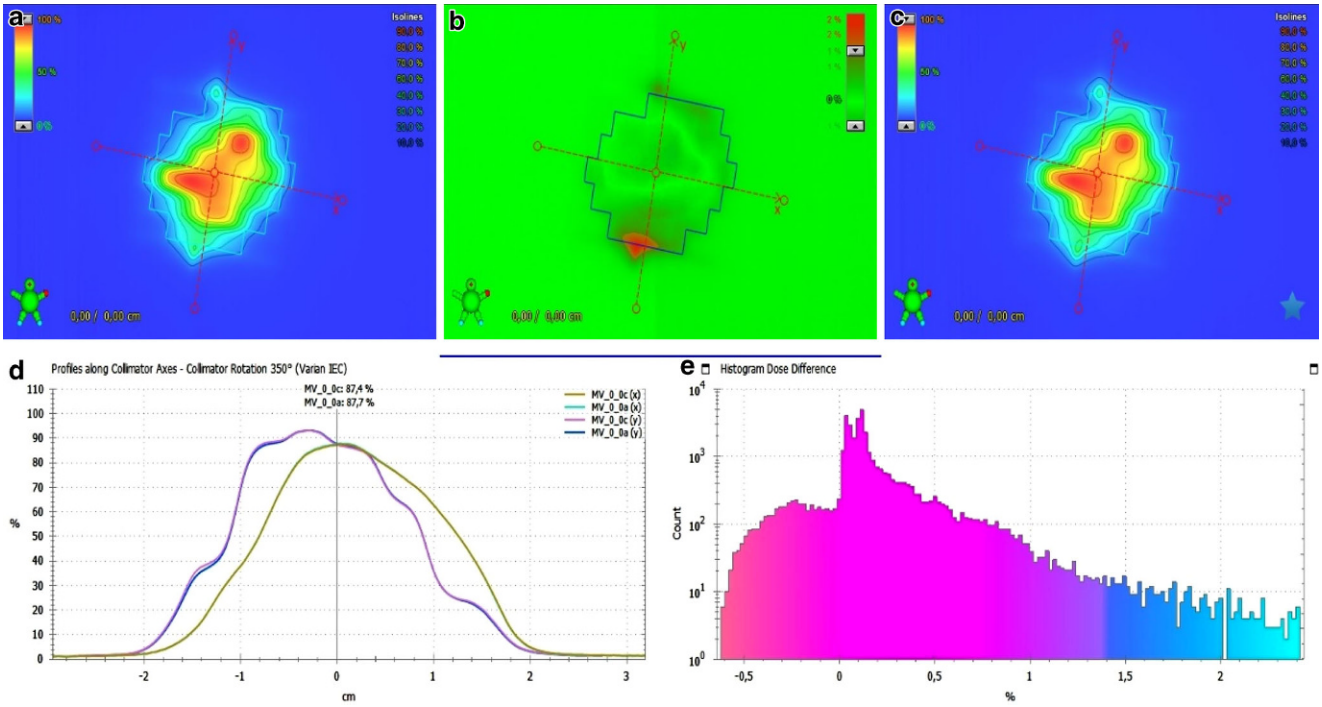

Fig. 4 Comparison of EPID-measured planar dose distribution showing gamma evaluation results (**b**, **e**) between two different fractions (**a**, **c**) and line profile agreement (**d**) for an arc of VMAT technique

of the other fractions by applying motion-simulated errors for the VMAT technique.

Patient irradiations were analyzed using 467 portal dosimetry images applying the ROI methods to every treatment field. PD results were retrospectively evaluated in relative and absolute mode. Table 4 summarizes %GPs obtained by comparison of each arc to the reference one (first fraction arc) in every fraction based on various criteria. All reviewed patient plans reached the clinical criteria for area gamma pass rate. Overall, %GPs were reduced by 3%/3 mm, 2%/2 mm, and 1%/1 mm criteria. For each criterion, the pass rate score was slightly decreased when

Table 4 Median passing rates for each fraction compared to the reference fraction, based on various criteria and regions of interest for VMAT technique in patient plans

Fraction pass rate	3%/3 mm			2%/2 mm		
	Field	*MLC-CIAO + 1 cm*	*MLC-CIAO + 1 cm (threshold 5%)*	*Field*	*MLC-CIAO + 1 cm*	*MLC-CIAO + 1 cm (threshold 5%)*
	Mean					
Fraction 2	98.96	97.43	96.90	97.77	95.47	93.71
Fraction 3	97.84	96.38	95.1	96.16	93.78	92.04
Fraction 4	98.55	98.19	97.95	97.49	96.90	96.38
Fraction 5	98.02	97.59	96.67	96.55	95.42	93.37

MLC-CIAO multi leaf collimator – complete irradiation area outline

Table 5 Nonparametric related samples Friedman's test two-way analysis results on patient plans

	Acceptance criteria (%/mm)					
	3%/3 mm		2%/2 mm		1%/1 mm	
	Asymp. Sig.	Exact Sig.	Asymp. Sig.	Exact Sig.	Asymp. Sig.	Exact Sig.
Field	0.392	0.442	0.830	0.846	0.559	0.578
MLC-CIAO + 1 cm	0.631	0.663	0.898	0.908	0.441	0.461
MLC-CIAO + 1 cm (threshold 5%)	0.903	0.915	0.661	0.677	0.615	0.645

MLC-CIAO multi leaf collimator – complete irradiation area outline, *asymp.* asymptotic, *sig.* significant

the MLC-CIAO + 1 cm was used instead of the field and more significantly for MLC-CIAO + 1 cm (threshold 5%).

There were noticeable changes in sensitivity for the 2%/2 mm criterion by using MLC-CIAO + 1 cm (threshold 5%) and a more significant reduction with 1%/1 mm. Neither asymptotic significant nor exact significant differences were found between all irradiated fractions and plans (Table 5). Statistical analysis showed that *p*-values for all comparisons, amongst three sets of DTA and DD as well as amongst sub-divisions of each criterion, are less than 0.001.

Discussion

In this study, we presented and assessed a relatively simple method for online verification of lung SBRT treatment. A rapid real-time transit dosimetry approach was investigated, which obtains information from EPID image data. Exit fluence variation due to patient intra- and inter-fractional anatomy changes were quantified using QUASAR™ phantom. The aim was to investigate the accuracy of synchronization of measured image sets during treatment deliveries, check prediction model accuracy for transit patient images using integrated image evaluation, check the initial results for patient treatment verification, and determine the challenges to clinical adoption of real-time transit EPID dosimetry systems.

This method is straightforward to perform and does not need any implementation of sophisticated analytical or EPID modelling approaches. We have performed detailed gamma analysis on 162 portal dose images for the phantom study. Gamma index analysis has been commonly implemented as an efficient tool in clinical routine [32, 33]. Thereby, it is essential to understand the limitations and sensitivity of the gamma method and the EPID. In order to determine the specificity of the system, we introduced deliberate errors and varied the gamma criteria. The results concern the detection threshold of simulated errors. In general, even if the EPID was designed for imaging, it was able to quantify errors when using tighter gamma tolerance than 3%/3 mm. Our results showed that the use of a combination of criteria might provide an effective way of improving the overall sensitivity of EPID. Gamma criteria of 2%/2 mm and 3%/3 mm are not sensitive in detecting motion errors for the VMAT technique. Thus, a stricter criterion (1%/1 mm) is needed to detect the motion-simulated errors. Primarily, it should be evaluated in local normalization, as summarized in Table 3. The results obtained in 3DCRT revealed that the 2%/2 mm criterion for any ROI in both local and improved normalization had sensitivity to any delivered inaccuracies.

The prevention of errors and the delivery of high-quality radiation treatments are basic principles in radiotherapy departments. The pre-treatment EPID dosimetry is suited for detecting only 6% of all the radiation therapy clinically reported incidents. In vivo EPID dosimetry was more skilled and was able to detect the majority (74%) of incidents related to radiotherapy [25], which obviously were not detected by pre-treatment dosimetry since the patient was not present in the beam. It was stated by Gardner et al., that in IMRT prostate patients, the largest variation in exit fluence due to machine delivery and patient anatomy-related sources are about 4.0% and 8.5%, respectively. Therefore, deviations caused by patient anatomy-related sources are slightly larger [34]. Moreover, regarding Thwaites et al.'s recommendation, an approach that can detect variations in tumor motion would be a useful treatment verification tool [35]. A further study from the Netherlands Cancer Institute disclosed that 9 out of 17 serious errors recognized in 4337 patients would have been missed without in vivo verification of radiation delivery [23]. Ultimately, EPID in vivo dosimetry for post-treatment inspections has been performed by a few institutions [36–39]. In the near future, the authors aim to reconstruct the EPID images with precise algorithms and provide 3D dose distribution, which can be compared with the planned dose. Some recent works have enabled measured images by back-projecting to planes or volumes within the patient, so the dose inside the patient can be reconstructed in 2D [40].

We observed that the changes in dose distribution could be recognized in small tumors (less than 5 cm) by tighter gamma evaluation, which were combined with ROI criteria. Consequently, local gamma evaluation should be considered for the VMAT technique to provide an effective way of improving the overall sensitivity of EPID.

In vivo dosimetry has been recognized as one of the next milestones in radiation oncology. We developed a patient rapid real-time transit dosimetry method with EPID, which is validated for hypofractionated treatments with FFF beams, as a step toward EPID in vivo dosimetry. The approach introduced errors that can occur based on patient anatomy. As described in the previous sections, we chose various treatment planning techniques to see if there were any differences in the result. The intent was not to describe every source of deviation, but to show the potential Achilles heel of pre-treatment QA measurements. By increasing the use of SBRT combined with substantial dose deliveries in 1 to 5 fractions as well as the biological responses of tumor to radiation, there is a high need for monitoring systems and detecting treatment delivery errors. In this work the obtained EPID images in each fraction were compared to the baseline in order to interpret the exit dosimetry. It is sensitive enough to provide useful information about the reproducibility of treatment delivery and patient setup. The

results demonstrate that PD is efficient and feasible under certain circumstances for detecting errors. The commonly used criterion of 3%/3 mm was inadequate for discovering target motion errors.

Further work is required to develop a real-time verification system which provides an additional tool that can assist with the prevention of significant mistreatments in radiation therapy. In vivo portal dosimetry can be used to calculate the dose distribution within the patient based on images acquired during treatment [20, 41]. Obviously, in vivo dosimetry improves the potential of detecting delivery errors, but it is still limited in its capacity to prevent errors before clinically significant errors occur [42].

Conclusion

This study demonstrates the feasibility of EPID for detecting the interplay effects. We recommend using thin computed tomography slices and adding sufficient tumor margin in order to limit the dosimetric organ motion in hypofractionated irradiation with preserved plan quality. In the presence of respiratory and gastrointestinal motion, tighter criteria and consequently using local gamma evaluation should be considered, especially for VMAT. This methodology offers a substantial step forward for in vivo dosimetry and the potential to distinguish errors depending on the gamma tolerances. Thus, the approach/prototype provides a fast and easy QA procedure for treatment delivery verification.

New software generations will allow reconstruction of the dose inside the patient and, if errors are found, will analyze their clinical relevance. EPID in vivo dosimetry will be a milestone of treatment planning QA, following the clinical improvement.

Compliance with ethical guidelines

Conflict of interest C. Moustakis, F. Ebrahimi Tazehmahalleh, K. Elsayad, F. Fezeu, and S. Scobioala declare that they have no competing interests.

Ethical standards For this article, no studies with human participants or animals were performed by any of the authors. All procedures performed were in accordance with the ethical standards of the institutional and/or national research committee and with the 1964 Helsinki declaration and its later amendments or comparable ethical standards.

References

1. Martel MK, Ten Hauken RK, Hazuka MB, Kessler ML, Strawderman M, Turrisi AT et al (1999) Estimation of tumor control probability model parameters from 3-D dose distributions of non-small cell lung cancer patients. Lung Cancer 24(1):31–37
2. Robertson JM, Ten Haken RK, Hazuka MB, Turrisi AT, Martel MK, Pu AT et al (1997) Dose escalation for non-small cell lung cancer using conformal radiation therapy. Int J Radiat Oncol Biol Phys 37(5):1079–1085
3. Sveistrup J, Rosenschold PM, Deasy JO, Oh JH, Pommer T, Petersen PM et al (2014) Improvement in toxicity in high risk prostate cancer patients treated with image-guided intensity-modulated radiotherapy compared to 3D conformal radiotherapy without daily image guidance. Radiat Oncol 9:44
4. Chung HT, Lee B, Park E, Lu JJ, Xia P (2008) Can all centers plan intensity-modulated radiotherapy (IMRT) effectively? An external audit of dosimetric comparisons between three-dimensional conformal radiotherapy and IMRT for adjuvant chemoradiation for gastric cancer. Int J Radiat Oncol Biol Phys 71(4):1167–1174
5. Williams MJ, Bailey M, Forstner D, Metcalfe PE (2007) Multicentre quality assurance of intensity-modulated radiation therapy plans: a precursor to clinical trials. Australas Radiol 51(5):472–479
6. Moore KL, Brame RS, Low DA, Mutic S (2012) Quantitative metrics for assessing plan quality. Semin Radiat Oncol 22(1):62–69
7. Yuan L, Ge Y, Lee WR, Yin FF, Kirkpatrick JP, Wu QJ (2012) Quantitative analysis of the factors which affect the interpatient organ-at-risk dose sparing variation in IMRT plans. Med Phys 39(11):6868–6878
8. Hunt MA, Jackson A, Narayana A, Lee N (2006) Geometric factors influencing dosimetric sparing of the parotid glands using IMRT. Int J Radiat Oncol Biol Phys 66((1):296–304
9. Wu B, Ricchetti F, Sanguineti G, Kazhdan M, Simari P, Chuang M et al (2009) Patient geometry-driven information retrieval for IMRT treatment plan quality control. Med Phys 36(12):5497
10. Moustakis C, Blanck O, Ebrahimi Tazehmahalleh F, Heng KCM, Ernst I, Krieger T et al (2017) Planning benchmark study for SBRT of early stage NSCLC: results of the DEGRO Working Group Stereotactic Radiotherapy. Strahlenther Onkol 193(10):780–790
11. Mans A, Wendling M, McDermott L, Sonke J-J, Tielenburg R, Vijlbrief R et al (2010) Catching errors with in vivo EPID dosimetry. Med Phys 37(6):2638–2644
12. Huang G, Medlam G, Lee J, Billingsley S, Bissonnette J-P, Ringash J et al (2005) Error in the delivery of radiation therapy: results of a quality assurance review. Int J Radiat Oncol Biol Phys 61(5):1590–1595
13. Patton GA, Gaffney DK, Moeller JH (2003) Facilitation of radiotherapeutic error by computerized record and verify systems. Int J Radiat Oncol Biol Phys 56(1):50–57
14. Van Herk M (2004) Errors and margin. Semin Radiat Oncol 14(1):52–64
15. Liu HH, Balter P, Tutt T, Choi B, Zhang J, Wang C et al (2007) Assessing respiration-induced tumor motion and internal target volume using four-dimensional computed tomography for radiotherapy of lung cancer. Int J Radiat Oncol Biol Phys 68(2):531–540
16. Seppenwoolde Y, Shirato H, Kitamura K, Shimizu S, van Herk M, Lebesque JV et al (2002) Precise and realtime measurement of 3D tumor motion in lung due to breathing and heartbeat, measured during radiotherapy. Int J Radiat Oncol Biol Phys 53(4):822–834
17. Xu F, Wang J, Bai S, Li Y, Shen Y, Zhong R et al (2008) Detection of intrafractional tumour position error in radiotherapy utilizing cone beam computed tomography. Radiother Oncol 89(3):311–319
18. Gauer T, Sothmann Th, Blanck O, Petersen C, Werner C (2018) Under-reported dosimetry errors due to interplay effects during VMAT dose delivery in extreme hypofractionated stereotactic radiotherapy. Strahlenther Onkol 194(6):570–579
19. Hoogeman MS, Nuyttens JJ, Levendag PC, Heijmen BJ (2008) Time dependence of intrafraction patient motion assessed by repeat stereoscopic imaging. Int J Radiat Oncol Biol Phys 70(2):609–618
20. McDermott LN, Wendling M, Sonke J-J, van Herk M, Mijnheer BJ (2007) Replacing pretreatment verification with in vivo EPID dosimetry for prostate IMRT. Int J Radiat Oncol Biol Phys 67(5):1568–1577

21. Piermattei A, Greco F, Azario L, Porcelli A, Cilla S, Zucca S et al (2012) A national project for in vivo dosimetry procedures in radiotherapy: first results. Nucl Instrum Methods Phys Res B 274:42–50
22. Defoor DL, Vazquez-Quino LA, Mavroidis P, Papanikolaou N, Stathakis S (2015) Anatomy-based, patient specific VMAT QA using EPID or MLC log files. J Appl Clin Med Phys 16(3):5283
23. Mijnheer B, Olaciregui-Ruiz I, Rozendaal R, Spreeuw H, van Herk M, Mans A (2015) Current status of 3D EPID-based in vivo dosimetry in The Netherlands Cancer Institute. J Phys Conf Ser. https://doi.org/10.1088/1742-6596/573/1/012014
24. Rowshanfarzad P, Mcgarry CK, Barnes MP, Sabet M, Ebert MA (2014) An EPID-based method for comprehensive verification of gantry EPID and the MLC carriage positional accuracy in Varian linacs during arc treatments. Radiat Oncol 9(1):249–259
25. Bojechko C, Phillps M, Kalet A, Ford EC (2015) A quantification of the effectiveness of EPID dosimetry and software-based plan verification systems in detecting incidents in radiotherapy. Med Phys 42(9):5363–5369
26. Quino LAV, Chen X, Fitzpatrick M, Shi C, Stathakis S, Gutierrez A et al (2014) Patient specific pretreatment QA verification using an EPID approach. Technol Cancer Res Treat 13(1):1–10
27. International Atomic Energy Agency (2012) Development of procedures for in vivo dosimetry in radiotherapy. Human health report no. 8. IAEA, Vienna
28. Nijsten SM, Mijnheer BJ, Dekker AL, Lambin P, Minken AW (2007) Routine individualised patient dosimetry using electronic portal imaging devices. Radiother Oncol 83(1):65–75
29. Keall PJ, Mageras GS, Balter JM, Emery RS, Forster KM, Jiang SB et al (2006) The management of respiratory motion in radiation oncology report of AAPM Task Group 76. Med Phys 33(10):3874–3900
30. Seuntjens J, Lartigau EF, Cora S, Ding GX, Goetsch S, Nuyttens J et al (2014) Prescribing, recording, and reporting of stereotactic treatments with small photon beams. J ICRU 14:1–160
31. Sterzing F, Brunner TB, Ernst I, Baus WW, Greve B, Herfarth K et al (2014) Stereotactic body radiotherapy for liver tumors: principles and practical guidelines of the DEGRO Working Group on Stereotactic Radiotherapy. Strahlenther Onkol 190:872–881
32. Van de Werf E, Lievens Y, Verstraete J, Pauwels K, Van de Bogaert W (2009) Time and motion study of radiotherapy delivery: economic burden of increased quality assurance and IMRT. Radiother Oncol 93(1):137–140
33. Hussein M, Tsang Y, Thomas RA, Gouldstone C, Maughan D, Snaith JA et al (2013) A methodology for dosimetry audit of rotational radiotherapy using a commercial detector array. Radiother Oncol 108(1):78–85
34. Gardner JK, Clews L, Gordon JJ, Wang S, Greer PB, Siebers JV (2009) Comparison of sources of exit fluence variation for IMRT. Phys Med Biol 54(19):N451–8
35. Thwaites DI, Verellen D (2010) Vorsprung durch Technik: evolution, implementation, QA and safety of new technology in radiotherapy. Radiother Oncol 94(2):125–128
36. van Elmpt W, McDermott L, Nijsten S, Wendling M, Lambin P, Mijnheer BJ (2008) A literature review of electronic portal imaging for radiotherapy dosimetry. Radiother Oncol 88(3):289–309
37. Mijnheer B, Beddar S, Izewska J, Reft C (2013) In vivo dosimetry in external beam radiotherapy. Med Phys 40(7):70903
38. Berry SL, Sheu RD, Polvorosa CS, Wuu CS (2012) Implementation of EPID transit dosimetry based on a through-air dosimetry algorithm. Med Phys 39(1):87–98
39. Berry SL, Polvorosa C, Cheng S, Deutsch I, Chao KS, Wuu CS (2014) Initial clinical experience performing patient treatment verification with an electronic portal imaging device transit dosimeter. Int J Radiat Oncol Biol Phys 88(1):204–209
40. Peca S, Brown DW (2014) Two-dimensional in vivo dose verification using portal imaging and correlation ratios. J Appl Clin Med Phys 15(4):117–128
41. Chan MKH, Leung RWK, Lee VWY, Wong MYP, Chiang CL, Law GML et al (2019) Linking dose delivery accuracy and planning target margin in radiosurgery based on dose-volume histograms derived from measurement-guided dose reconstruction. Phys Med Biol 64(4):045009. https://doi.org/10.1088/1361-6560/aafd47
42. Persoon L, Nijsten S, Wilbrink F, Podesta M, Snaith J, Lustberg T et al (2012) Interfractional trend analysis of dose differences based on 2D transit portal dosimetry. Phys Med Biol 57(20):6445–6458